

Taylor & Francis
Taylor & Francis Group

Plastics, Rubber and Composites
Macromolecular Engineering

ISSN: 1465-8011 (Print) 1743-2898 (Online) Journal homepage: http://www.tandfonline.com/loi/yprc20

Measurement of oxygen diffusion in PS/PNIPAM films using fluorescence quenching

Ö. Yargi, Ö. Pekcan & Ş. Uğur

To cite this article: Ö. Yargi, Ö. Pekcan & Ş. Uğur (2015) Measurement of oxygen diffusion in PS/PNIPAM films using fluorescence quenching, Plastics, Rubber and Composites, 44:5, 189-196, DOI: 10.1179/1743289815Y.0000000010

To link to this article: http://dx.doi.org/10.1179/1743289815Y.0000000010

Published online: 05 May 2015.

Submit your article to this journal

Article views: 44

View related articles

View Crossmark data

Full Terms & Conditions of access and use can be found at
http://www.tandfonline.com/action/journalInformation?journalCode=yprc20

Download by: [New York University] **Date:** 17 April 2016, At: 17:28

Measurement of oxygen diffusion in PS/PNIPAM films using fluorescence quenching

Ö. Yargi[1], Ö. Pekcan[2] and Ş. Uğur*[3]

The diffusion of oxygen into pyrene labelled polystyrene (PS) latex/poly(*N*-isopropylacrylamide) (PNIPAM) composite films (PS/PNIPAM) was studied based on PS content with the use of fluorescence quenching method. Fluorescence experiments were carried out on composite films containing pyrene as a sensor dye. The Stern–Volmer equation for fluorescence quenching is combined with Fick's law for diffusion to derive mathematical expressions. Diffusion coefficients (*D*) were produced and found to be decreased with increasing PS content. This decrease was explained with the formation of a tortuous path for diffusing gas molecules, which extends the diffusion path of oxygen in the films. In addition, at high PS content, two different *D* values were obtained, which were attributed to the existence of two different areas in the composite films.

Keywords: PS latex, PNIPAM latex, Fluorescence, Quenching, Oxygen, Diffusion, Composites, Films

Downloaded by [New York University] at 17:28 17 April 2016

Introduction

In the last two decades, it has been well established that hydrogels play an important role in living systems and are of broad interest for a large variety of industrial products.[1–4] These gels can be regarded as intermediates between solids and liquids, a property that manifests itself in a rather complex mixture of the properties of these limiting states. Thermosensitive systems like poly(*N*-isopropylacrylamide) (PNIPAM), hydrogels have attracted much attention,[5] because the viscoelastic characteristics can easily be controlled by changing the temperature. On the other hand, the bioadhesive properties of these materials point to possible applications as drug delivery systems in pharmaceutical applications. In aqueous solution, PNIPAM exhibits a lower critical solution temperature (LCST) between 30 and 35°C that results in a reversible transformation from a hydrophilic polymer to one that is hydrophobic as the solution temperature is raised above the LCST. With an LCST close to the normal body temperature, the thermosensitive nature of PNIPAM has resulted in a wide number of investigations for potential use in drug delivery systems.[6,7] In thin film geometry, such gels are of interest for applications such as thermosensitive surfaces, artificial pump and muscles, light modulation systems, and optical switches.

Composites based on hydrogels have shown many exciting properties. An actuation system based on submicrometre sized silicon columns with a hydrogel layer was used to show humidity responsive behavior.[8] As hydrogels are normally temperature responsive polymers, such composites may also present useful temperature sensitive properties. PNIPAM was chosen because it is one of the most popular and intensively studied hydrogels, and has found wide applications in many fields. It was reported that PNIPAM may have limited potential as a biomaterial,[9,10] and PLGA/MIx-PNIPAM thermoresponsive dispersions can be used as an injectable highly porous biodegradable cell delivery system. Several investigations have incorporated PNIPAM into aqueous core–shell nanoparticles, for which diverse thermally responsive properties can be obtained.[11,12] For many hydrogel applications, biocompatibility is also required and the material must also have high oxygen permeability, water sorption and wettability.[13–15] Most of these properties are interrelated. For example, oxygen permeability is largely related to water content and also influences biocompatibility. Oxygen is one of the most important reactants to be considered in the diffusion phenomenon. The control of the diffusion of oxygen is of particular importance in polymer oxidative degradation, protective coatings, and the design of polymeric membranes for separation processes in production of films for packing industry and in the developments of biocompatible materials.

For more than 50 years, polymer scientists have been interested in the influence of fillers on gas diffusion through polymer membrane.[16–20] Lu *et al.*[18] examined the influence of 10 nm diameter silica particles on oxygen diffusion in PDMS polymer film. A decrease was observed in oxygen diffusion coefficients, *D*, with increasing silica content. This reduction in *D* was attributed to the tortuous path for diffusing gas molecules and reduced molecular mobility of polymer chains caused by the filler particles. Bharadwaj[19] also addressed the modelling of gas barrier properties in polymer layered silicate nanocomposites based on a tortuosity argument. It was considered that the presence of filler introduces a tortuous path for a diffusing penetrant. The reduction of permeability arises from the longer diffusive path where the penetrants must travel in the presence of the layered silicate. Villaluenga *et al.*[20] investigated the

[1]Department of Physics, Yildiz Technical University, Istanbul, Turkey
[2]Kadir Has University, Cibali, Istanbul, Turkey
[3]Department of Physics, Istanbul Technical University, Istanbul, Turkey

*Corresponding author, email saziye@itu.edu.tr

© Institute of Materials, Minerals and Mining 2015
Published by Maney on behalf of the Institute
Received 21 January 2015; accepted 05 April 2015
DOI 10.1179/1743289815Y.0000000010

Downloaded by [New York University] at 17:28 17 April 2016

permeability, diffusivity and solubility of helium, oxygen and nitrogen in the unfilled and filled polypropylene (PP) membranes with montmorillonite clay using X-ray diffraction, thermogravimetric analyser, tensile testing and differential scanning calorimetry. They found that the filled membranes exhibited lower gas permeability compared to the unfilled PP membrane, and both diffusivity and solubility decreased by the presence of fillers. This reduction was interpreted in terms of the decrease in available free volume in the polymer, providing less sorption sites for gas molecules.

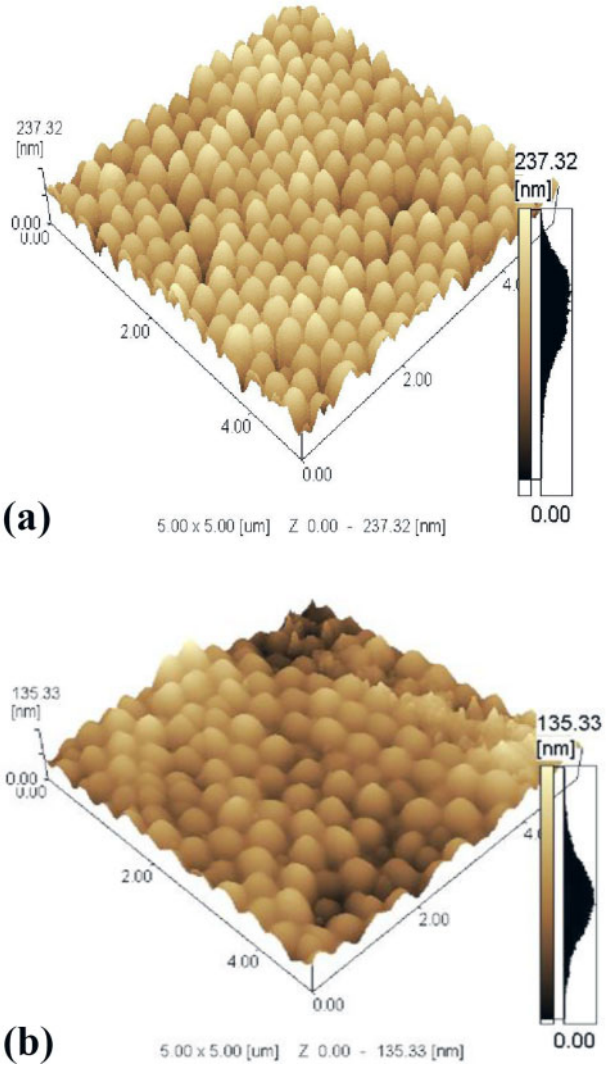
The usual procedure used to measure the diffusion coefficients of gases through a polymeric system is based on the measurements of the amount of gas that permeates a given area of polymer in a given time. One exposes one side of the polymer film to oxygen at time zero and measures the flux of oxygen across the film as a function of time. Knowing the dimensions of the film and the partial pressure of oxygen on the high pressure side, one can calculate the diffusion coefficient from the flux.[21] The diffusion coefficient of oxygen is determined from the kinetics of the approach of the oxygen flux to its steady state. Since oxygen is such a powerful quencher of fluorescence and phosphorescence, there is a natural attraction to using this property to determine this value. Another approach was also employed by Cox and Dunn[22] for studying large samples.[22] Here, one constructs a square cell with centimetre scale height. The cell is filled with a polymer containing the dye, and all the oxygen is removed. Cox irradiated a thin (1 mm) middle cross-section of the cell and then allowed oxygen to diffuse into the cell from the top. As the oxygen concentration profile propagates through the illuminated middle slice, the emission intensity is quenched. Cox and Dunn[22,23] and MacCallum and Rudkin[24] measured the oxygen diffusion coefficient by fluorescence quenching in planar sheets of poly(dimethyl siloxane),[22] filled poly(dimethyl siloxane) sample[23] and polystyrene (PS).[24] They monitored oxygen quenching of a fluorophore as a function of time by assuming that fluorophore dispersed homogeneously within the films. The mathematical determination of D varied, but the single underlying assumption in all cases was that the time dependent emission intensity was measured during the experiment. In some cases, the intensity versus time curve was converted to a concentration versus time curve using the Stern–Volmer relationship.[22,23] Winnik and Manners[25,26] have used time scan experiments to measure the decay of luminescence intensity as oxygen diffuses into polymer films under constant illumination and the growth of intensity as oxygen diffuses out of the film. They interpreted their data with the aid of theoretical models based on Stern–Volmer quenching kinetics with Fick's laws of diffusion. In some of our earlier studies, we examined the effect of annealing,[27] packing,[26] clay and CNT contents[29,30] and temperature[31,32] on the oxygen diffusion coefficient, D, in poly(methyl methacrylate) by using steady state and photon transmission techniques.

In this work, the diffusion behaviour of oxygen into PS/PNIPAM composite films was studied depending on the PS content. Six different sets of composite films were prepared from pyrene labelled PS latex and PNIPAM microgel mixtures with 5, 10, 15, 25, 40 and 60 wt-% PS content drying at room temperature. Fluorescence quenching technique was used to study oxygen diffusion into these composite films at room temperature. The intensity change of excited pyrene was monitored during the oxygen penetration into composite films. A model was developed for low quenching efficiency to measure the oxygen diffusion coefficient, D.

Experimental

PS latex particles

Pyrene labelled PS particles were produced via surfactant free emulsion polymerisation process.[33] The polymerisation was performed batch wisely using a thermostated reactor equipped with a condenser, thermocouple, mechanical stirring paddle and nitrogen inlet. The agitation rate was 400 rev min^{-1}, and the polymerisation temperature was controlled at 70°C. Water (100 mL) and styrene (5 g) were first mixed in the polymerisation reactor, where the temperature was kept constant (at 70°C). Potassium peroxodisulphate (KPS) initiator (0·1 g) dissolved in small amount of water (2 mL) was then introduced in order to induce styrene polymerisation. The polymerisation was conducted during 18 h. The polymer has a high glass transition temperature ($T_g = 105$°C). The latex dispersion has an average particle size of 400 nm. Figure 1*a* shows the atomic force micrograph (AFM) image of PS latex particles produced for this study.



1 AFM images of *a* PS and *b* PNIPAM latex particles

Downloaded by [New York University] at 17:28 17 April 2016

PNIPAM particles

PNIPAM microgel particles were synthesised via precipitation polymerisation process.[34] N-isopropylacrylamide (NIPAM) from Kodak was purified using a 60/40 (v/v) of hexane and toluene mixtures. Methylene bisacrylamide (MBA) from Aldrich was used as crosslinker monomer and was used as received. Fluorescent monomer 1-pyrenylmethacrylate (PolyFluor^{TM} 394) was from Polysciences Inc. and was used as such. The polymerisation was performed using 1·2 g NIPAM, 0·059 g MBA and 0·018 g KPS as the initiator. All the reactants were first solubilised in water and introduced in the polymerisation reactor. The polymerisation was conducted (in 50 mL deionised water) under nitrogen atmosphere and at 70°C. The polymerisation reaction was carried out in 100 mL four-neck glass reactor equipped with a glass anchor type agitation (200 rev min^{-1}), a condenser and a nitrogen inlet. The polymerisation reaction was conducted for 16 h. The final conversion was gravimetrically determined and found to be 98·5%. The mean diameter of synthesised PNIPAM particles is 320 nm, and their T_g is 135°C. Figure 1*b* shows the AFM image of pure PNIPAM latex used in this study.

Preparation of PS doped PNIPAM (PS/PNIPAM) films

PS/PNIPAM composite films were prepared by the casting method. Six different films with 5, 10, 15, 25, 40 and 60 wt-% PS content were prepared from the mixture of PNIPAM and PS dispersion by using the relation $W_{PS}(\text{wt-}\%) = (W_{PS}/(W_{PS} + W_{PNIPAM})) \times 100$, where W_{PS} and W_{PNIPAM} are the weight of PNIPAM and PS latex respectively. By placing the same number of drops on a glass plate of $0{\cdot}8 \times 2{\cdot}5$ cm^2 and allowing the water to evaporate, dry films were obtained. Film thickness was measured ~8 μm. Figure 2 presents the AFMs of 5 and 20 wt-% PS content composite films respectively.

Fluorescence measurements

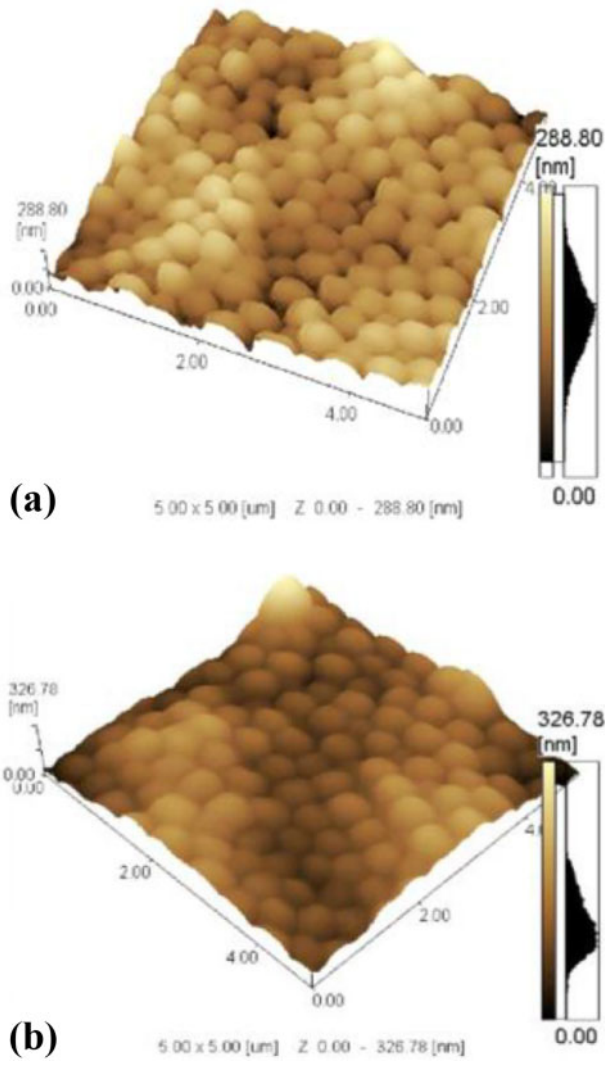
Fluorescence measurements were carried out using a Perkin Elmer model LS-50 fluorescence spectrophotometer. Before fluorescence experiments, composite films were placed in a round quartz tube ($4{\cdot}0$ cm $\times$ $1{\cdot}0$ cm $\times$ $1{\cdot}0$ cm), and the tube was flushed with nitrogen until all of the oxygen was removed from the film (Fig. 3*a*). Then, the quartz tube was placed in the spectrophotometer and the films were illuminated with the 345 nm excitation light of pyrene. O_2 diffusion experiments were performed for each film sample at room temperature (24°C), and in all experiments, the maximum peak of 395 nm was used for the pyrene intensity (I_P) measurements. When these films are exposed to air, oxygen molecules penetrate into the films and the excited state of many pyrenes is rapidly quenched upon encountering an oxygen molecule. The key parameter for understanding the response of the system to the presence of oxygen, assuming diffusion controlled quenching, is the intensity of unquenched pyrenes. Thus, we monitor the fluorescence emission intensity of pyrene molecules to get information about the diffusion of oxygen into the film. The change in the pyrene intensity, I_P, was monitored against time, after the quartz tube was open to the air for (O_2) diffusion experiments by using time drive mode of spectrophotometer (Fig. 3*b*). All measurements were made at the 90° position, and the slit widths were kept at 8 nm. Since the diffusion measurements required that oxygen permeate only one surface of the film, a small region in the centre of the films was masked off for measurement using black tape on the opposite side of the samples. This was also done to prevent reflection of light.

Theoritical considerations

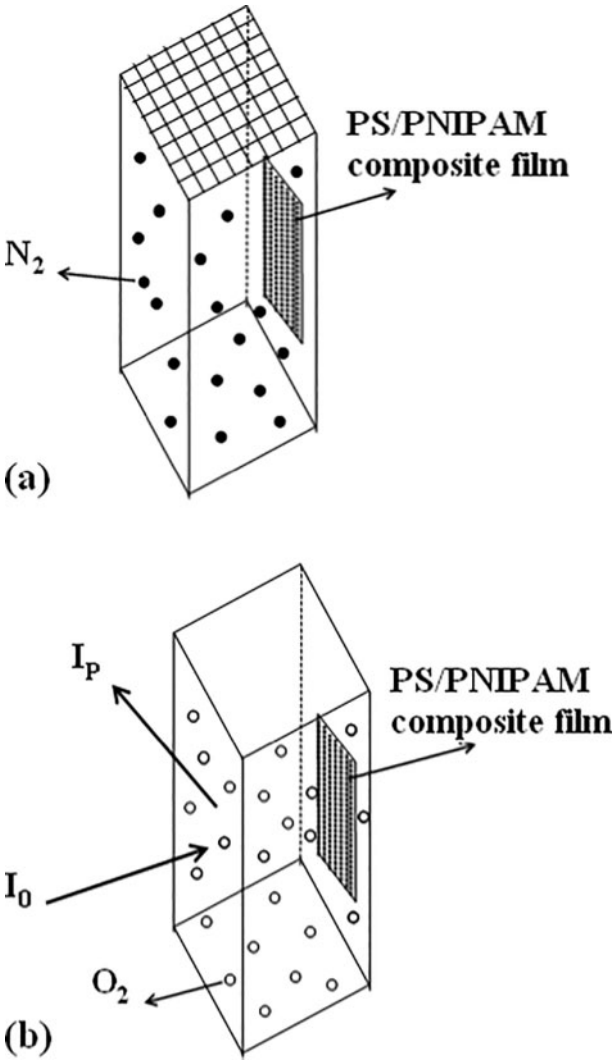
Fluorescence quenching by oxygen

When samples containing fluorescent probes are exposed to air or their solutions are saturated with oxygen, the fluorescence intensities of the samples decrease and the rates of fluorescence decay increase. These phenomena are due to oxygen quenching of the probe's excited state. The mechanism of quenching involves a sequence of spin allowed internal conversion process, which takes place within a weakly associated encounter complex between probe and oxygen. The product is either a singlet ground state or an excited triplet species.[29]

Data generated from oxygen quenching studies on small molecules in homogeneous solution are usually analysed using the Stern–Volmer relation, provided that the oxygen concentration (O_2(is not too high.[27]



2 AFM images of *a* 5 wt-% and *b* 20 wt-% PS composite films



3 Diffusion cell in the PerkinElmer LS-50 spectrofluorimeter: *a* diffusion cell filled with nitrogen; *b* diffusion cell exposed to air for oxygen diffusion; I_0 and I_P are excitation and emission intensities at 345 and 395 nm respectively; cartoon representation of oxygen diffusion into film at elevated time intervals

$$\frac{I_0}{I} = 1 + k_q \tau_0 [O_2] \quad (1)$$

In this equation, I and I_0 are the fluorescence intensities in the presence and absence of oxygen respectively, k_q is the bimolecular quenching rate constant and τ_0 is the fluorescence lifetime in the absence of O_2. This equation requires that the decay of fluorescence is single exponential and, moreover, that quenching interactions occur with a unique rate constant k_q. From the slope of a plot of I_0/I versus $[O_2]$, k_q can be determined provided that τ_0 is known. Diffusion coefficients related to the quenching events can be calculated from the time independent Smoluchowski–Einstein equation[27]

$$k_q = \frac{4\pi N_A (D_P + D_q) p R}{1000} \quad (2)$$

where D_P and D_q are diffusion coefficients of the excited probe and quencher respectively, p is the quenching probability per collision, R is the sum of the collision radii ($R_P + R_q$), and N_A is Avagadro's number. Equations (1) and (2) can also be applied to the case of quenching of polymer bound excited states in glass as long as the fluorescence decay is exponential and k_q is single valued. A simplifying factor in the interpretation of k_q is the general assumption that $D_P \ll D_q$ when the probe is covalently attached to a polymer. For quenchers as small as molecular oxygen, such an assumption would not be unwarranted. On the time scale of fluorescence, the overall translational diffusion coefficient of the polymer coil is usually not important; the relevant diffusion coefficient is that for motion of individual chain segments.

Diffusion in plane sheet

When Fick's second law of diffusion is applied to plane sheet and solved by assuming a constant diffusion coefficient, the following equation is obtained for concentration changes in time[28]

$$\frac{C}{C_0} = \frac{x}{d} + \frac{2}{\pi}\sum_{n=1}^{\infty} \frac{\cos n\pi}{n} \sin \frac{n\pi x}{d} \exp\left(-\frac{Dn^2\pi^2 t}{d^2}\right) \quad (3)$$

where d is the thickness of the slab, D is the diffusion coefficient of the diffusant, and C_0 and C are the concentration of the diffusant at time zero and t respectively; x corresponds to the distance at which C is measured. We can replace the concentration terms with the amount of the diffusant by using equation (4)

$$M = \int_V C dV \quad (4)$$

When equation (4) is considered for a plane volume element and substituted in equation (3), the following solution is obtained[26]:

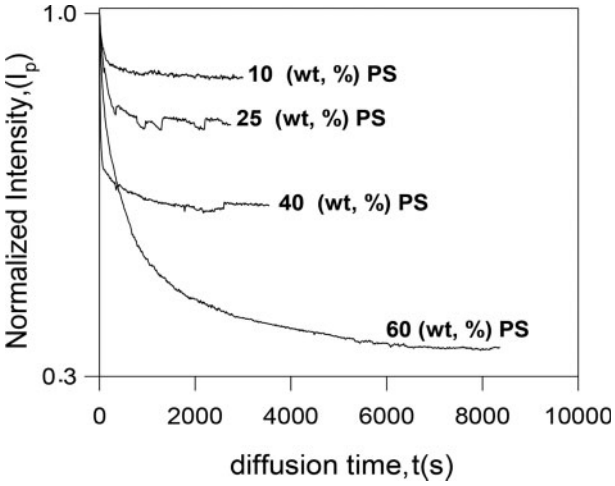
$$\frac{M_t}{M_\infty} = 1 - \frac{8}{\pi^2}\sum_{n=0}^{\infty} \frac{1}{(2n+1)^2} \exp\left(-\frac{D(2n+1)^2\pi^2 t}{d^2}\right) \quad (5)$$

where M_t and M_∞ represent the amounts of diffusant entering the plane sheet at time t and infinity respectively.

Results and discussion

In Fig. 4, normalised pyrene intensity, I_P, curves are presented against diffusion time for films having different PS content exposed to oxygen. It is seen that, for all film samples, oxygen diffusion began as soon as the films are exposed to air. As oxygen diffused through the planar film, the emission intensity of the pyrene decreased according to equation (1) for each PS content film and was saturated once oxygen equilibrated in the film. Here, it has to be noted that this saturation process is completed at shorter times for low (10 and 25 wt-%) PS content films showing rapid diffusion of O_2 molecules into these films. Whereas for high (40 and 60 wt-%) PS content films, the saturation process takes longer time, showing that O_2 diffusion is slowing down. In addition, the quenching rate increases with increasing PS content in the film predicting the more rapid quenching of excited pyrenes by O_2 molecules, diffused into the films. The curves reached their equilibrium values almost

Downloaded by [New York University] at 17:28 17 April 2016

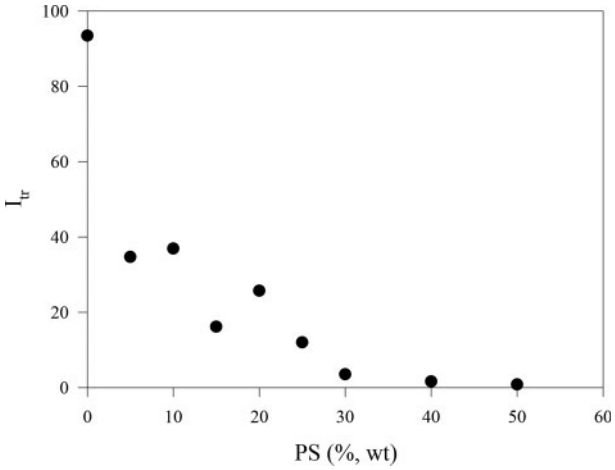


4 Time behaviour of pyrene, P, and fluorescence intensity, I_P, during oxygen diffusion into PS/PNIPAM composite films with different PS content; numbers on each curve indicate PS content (wt-%) in film

in the same fashion as oxygen diffused through and equilibrated in the film.

In many applications, optical transparency is also important for gas diffusion into composite films. Figure 5 presents the plot of the transmitted light intensity (I_{tr}) (measured at 500 nm) versus PS content at room temperature.[35] It is seen that inclusion of PS into PNIPAM lattice strongly decreases the transmitted light intensity, I_{tr}. As the PS concentration increases from 0 to 5 wt-%, light transmission decreases rapidly from 95 to 35%. I_{tr} decreased to very low values with increasing PS content and drops to the lowest value at 30 wt-% PS content. Neither PNIPAM nor PS has a significant absorption at the 500 nm wavelength. So, this decrease can be explained with the phase separation process between PNIPAM and PS particles, which creates lattice heterogeneities in the film, resulting in increased light scattering and low transparency. As PS content is increased, PS particles percolate in PNIPAM lattice, and at 30 wt-%, the largest cluster of PS appears by connecting the left and right edges to the bottom edge of the PNIPAM lattice.[35]

In the light of this explanation, the behaviour of I_P can be made as follows: Since low PS content films possess many



5 Plot of transmitted light intensities versus PS latex content

voids (*see* Fig. 2), oxygen molecules diffuse easily into films through these voids. The rapid diffusion of O_2 molecules into the films through these voids causes the saturation of I_P at shorter times due to the short diffusion path perpendicular to the thickness direction of the film. The short diffusion path also reduces the possibility of O_2 molecules to meet the excited pyrene molecules in the composite film, which results in a low quenching rate but a short diffusion time. On the other hand, the higher rate of quenching and the longer diffusion time at high PS content can be explained with the formation of the percolation cluster of PS in PNIPAM matrix as explained above. In this percolating cluster, because the PS particles are densely packed, they create an extremely tortuous pathway that significantly increases both the diffusion path and the residence time of diffusing O_2 molecules in the films. This gives O_2 molecules more chance to meet the excited pyrene molecules in the composite film, resulting in high quenching rate but long diffusion time.

This result is consistent with microstructural analysis. AFM images of composite films with 5 and 20 wt-% PS content in Fig. 2 also confirm this picture. It can be seen that there is a very high proportion of pores present in 5 wt-% PS content film in comparison with 20 wt-% PS content film. Increasing the PS content seems to lead to a more homogenous and smooth film structure due to the highly ordered PS particles, creating an extended diffusion pathway for O_2 molecules, which dramatically reduce oxygen diffusion rate.

In order to interpret the above findings, equation (1) can be used by expanding in a series for low quenching efficiency, i.e. $k_q\tau_0[O_2] \ll 1$, which then produces the following useful result:

$$I \approx I_0(1 - k_q\tau_0[O_2]) \tag{6}$$

During O_2 diffusion into the latex films, pyrene molecules are quenched in the volume, which is occupied by O_2 molecules at time t. Then, pyrene intensity at time t can be represented by the volume integration of equation (6) as

$$I_t = \frac{\int I dv}{\int dv} = I_0 - \frac{k_q\tau_0 I_0}{V}\int dv[O_2] \tag{7}$$

where dv and V are the differential and total volume of composite film presented in Fig. 6. Performing the integration, the following relation is obtained

$$I_t = I_0\left(1 - k_q\frac{\tau_0}{V}O_2(t)\right) \tag{8}$$

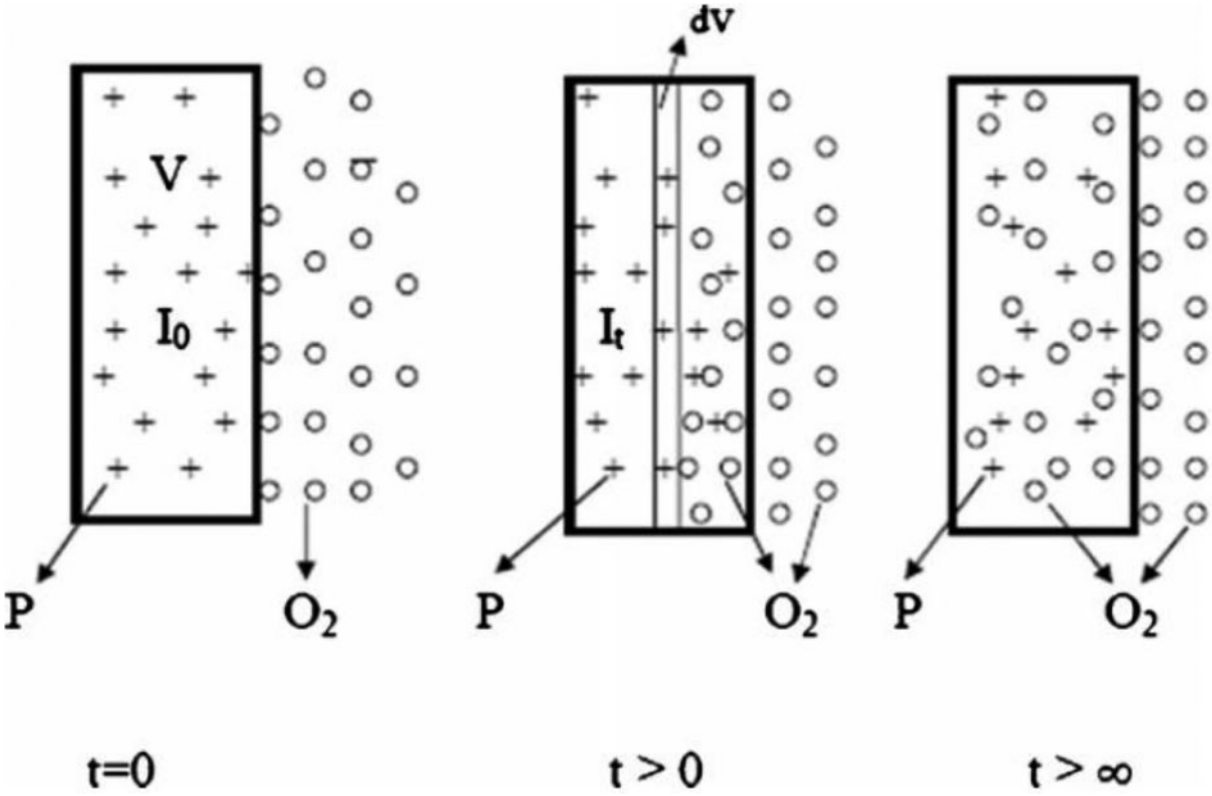
where $O_2(t) = \int dv[O_2]$ is the amount of oxygen molecules diffuse into latex film at time t.

Combining equation (8) with the Fick's law (equation (5)), the change in I_P due to the change in the oxygen concentration is related to the time. If it is assumed that $O_2(t)$ corresponds to M_t, then equation (8) can be combined with equation (5). Combining equation (8) for $n = 0$ for oxygen diffusion with equation (5), the following useful relation is obtained to interpret the diffusion curves in Fig. 4

$$\frac{I_t}{I_0} = A + \frac{8C}{\pi^2}\exp\left(-\frac{D\pi^2 t}{d^2}\right) \tag{9}$$

where $C = (k_q\tau_0 O_2(\infty))/V$ and $A = 1 - C$. Here, $O_2(\infty)$ is the amount of oxygen molecules that diffuse into latex film

Downloaded by [New York University] at 17:28 17 April 2016



6 Cartoon representation of oxygen diffusion into latex film

Downloaded by [New York University] at 17:28 17 April 2016

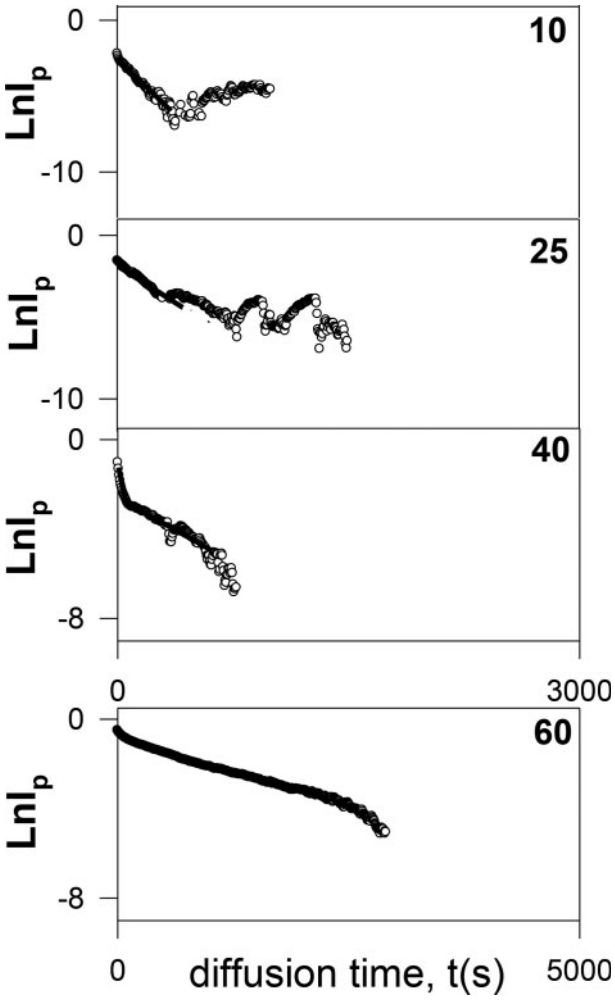
at time infinity. Now, this expression can be used to interpret the diffusion curves in Fig. 4. Here, by flushing the cell with nitrogen, the oxygen concentration was assumed to be zero both inside and outside of the film. Hence, the pyrene intensity is assumed to be maximum ($= I_0$) at the beginning. When the film was exposed to air at time zero, while the O_2 concentration increases to its final uniform equilibrium value inside the film, emission intensity decreases to its minimum equilibrium value. As a result, we combined the linear Stern–Volmer equation with the diffusion model to extract the diffusion coefficients from the experimental data. The logarithmic form of equation (9) can be written as follows:

$$\mathrm{Ln}\left(\frac{I_t}{I_0} - A\right) = \mathrm{Ln}\left(\frac{8C}{\pi^2}\right) - \frac{D\pi^2}{d^2}t \qquad (10)$$

Fig. 7 shows logarithmic plot of the data in Fig. 4 versus diffusion time for various PS content films. The solid lines represent the best fit to the diffusion model (equation (10)). A good fit of the experimental data to equation (10) confirms the applicability of a Fickian diffusion model for the material under consideration and hence the Fickian model adequate to characterise these composites for the O_2 diffusion. We can extract information about both k_q and D by fitting equation (10) to the data in Fig. 7 using a linear least squares fitting method. Here, k_q values were calculated using C values. Similar fittings were done for all of the film samples, and k_q and D values were produced as listed in Table 1. The average D values were determined from three or five measurements on different samples in each case, and the standard deviations on D values are also given in Table 1.

Although all diffusion curves in Fig. 4 follow Fickian diffusion model, the logarithmic plot of diffusion curves for high PS content films (*see* Fig. 7*c* and *d*) represents two different regimes at short and longer times at which two different linear curves are seen. When these linear curves in Fig. 7*c* and *d* are compared to computations using equation (10), two different diffusion coefficients, D_1 and D_2, for oxygen diffusion are obtained, which are listed in Table 1. Here, D_1 coefficients are attributed to O_2 diffusion in defects/voids that are present in the composite film due to the phase separation process between PS and PNIPAM, while D_2 coefficients are related to O_2 diffusion in the ordered PS phase. As seen from Table 1, the diffusion coefficients (D_2) decreased with increasing PS content, indicating that PS content strongly affects the oxygen diffusion. The highly ordered PS particles that form a percolating cluster in PNIPAM matrix, described above, creates an extremely tortuous path for diffusing oxygen molecules. Thus, oxygen must penetrate into this ordered phase by rerouting its path, which significantly extends the diffusion pathway of a gas molecule. This larger residence time of a diffusing oxygen molecule in the film yields lower diffusion coefficients as shown in Table 1.

These findings are consistent with the results in our previous work.[36] In the previous study,[36] the diffusion of O_2 into PS/PNIPAM composite films was studied depending on both temperature and PS content. It was seen that D coefficients are strongly dependent on both temperature and PS fraction in the film. Diffusion coefficient was increased with increase in temperature for low PS content films except for the 40 wt-% PS content sample. The variation of D with respect to temperature in low PS content films was explained with the presence of microvoids. It was seen that there is a very high proportion of pores present in these low PS content films. However, only a slight increase was seen



7 Logarithmic plots of data in Fig. 4 and their fits to equation (10) for *a* 10 wt-%, *b* 25 wt-%, *c* 40 wt-% and *d* 60 wt-% PS content films

in D values of 40 wt-% PS content film with respect to temperature where no lattice heterogeneities (microvoids) were detected.[36] On the other hand, D values for this study (10^{-10} cm^2 s^1) are found to be in the same order of magnitude than those previously obtained for PS/PNIPAM[36] and PS/MNaLB[27] composite films and one order larger than that of pure PMMA latex[27] matrix by using the same technique. This difference can be originating from the absence of voids in PMMA films due to the formation of a mechanically strong, void-free continuous matrix during annealing, which hinders the diffusive processes from the film surface.

Kneas *et al.*[37] studied the effect of silica on diffusion coefficients, D, of oxygen for pTMSMMA films. They found a two-fold decrease in D with increasing amounts of silica. They explained this decrease as a result of the strong adsorption of oxygen onto the hydrophobic amorphous silica particles due to their large surface area, which acts as a trap for oxygen molecules. Cox and Dunn[22,23] investigated the influence of temperature on the diffusion of oxygen into silica filled silicone films by using the fluorescence quenching method. Despite the increase in diffusion coefficients with temperature, they observed a decrease in D values with the increasing silica content. They explained the decrease in D by both obstacle effects of filler and oxygen adsorption on its surface. Sorrentino *et al.*[38] and Pereira de Abreu *et al.*[39] also reported that polymer–clay nanocomposites exhibit improved gas barrier properties, reducing the diffusion of oxygen and water vapour across the matrix and help in maintaining the quality of food for several months. Huang *et al.*[40] studied the penetration of H_2O and O_2 into a series of polyimide–silica, polyimide–clay, and polyimide–silica–clay composite materials in the form of both coating and film by electrochemical corrosion measurements, gas permeability analysis and UV–Vis transmission spectroscopy. They found that superior dispersion of clay platelets into a polymer matrix effectively increases the length of diffusion pathways for oxygen and water. Increasing the clay ratio in polymer would increase the length of diffusion pathway of H_2O and O_2 molecules. Kose *et al.*[41] studied the morphology and luminescence oxygen sensor properties of blend films consisting of Ir-PDMS and PS by using fluorescence microscopy, atomic force microscopy and scanning electron microscopy. By using these methods, they found that the oxygen permeability in the blend films is spatially heterogeneous. Their results show that the micrometre sized Ir-PMDS domains display a two- to three-fold higher oxygen sensor response compared to the surrounding PS matrix, indicating that PDMS is considerably more gas permeable compared to PS.

When the pyrene diffusion in the latex film is omitted and $p = 1$ is taken, then equation (2) becomes

$$k_q = \frac{4\pi N_A D_m R}{1000} \tag{11}$$

Here, D_m is called as the mutual diffusion coefficient, which can now be assumed to be the self-diffusion coefficient of O_2 in the composite film. Since k_q is known and if R was taken as the radius of pyrene,[32] then the average D_m values were obtained and also listed in Table 1 for all film samples. From Table 1, it is seen that D_m is also dependent on the PS content in composite films and increases with increasing PS content. Two different D_m values for high PS content films refer to two different areas in composite films as stated above. Here, D_{m1} coefficient is attributed to O_2 diffusion in disordered areas (several kinds of defects/voids) of the

Table 1 Experimentally obtained diffusion (D) and mutual diffusion (D_m) coefficients

PS/wt-%	D_1 (cm^2 s^{-1}) $\times 10^{-10}$	D_2 (cm^2 s^{-1}) $\times 10^{-10}$	D_{m1} (cm^2 s^{-1}) $\times 10^{-5}$	D_{m2} (cm^2 s^{-1}) $\times 10^{-5}$
5	...	10±0.7	...	0.4±0.004
10	...	5.7±0.7	...	0.4±0.004
15	...	2.8±0.07	...	0.4±0.004
25	...	3.8±0.1	...	0.9±0.06
40	14±0.2			
	1.6±0.2	1.3±0.06	0.9±0.06	
60	3.7±0.2			
	1.3±0.2	2.2±0.1	1.3±0.1	

Downloaded by [New York University] at 17:28 17 April 2016

composite film, while D_{m2} coefficients are related to O_2 diffusion in highly ordered areas of the composite film. This behaviour also supports our explanation above related with the high quenching rate for high PS content films. The extension in the diffusion pathway of oxygen in high PS content films increases the possibility of oxygen molecules encountering a pyrene molecule in the excited state. Since D_m is directly proportional to k_q (see equation (11)), the increasing D_m values indicate that fluorescence quenching becomes more efficient with the increasing PS content.

Conclusions

This study illustrates that PS/PNIPAM nanocomposites have useful properties as fluorescent oxygen sensors, and a simple steady state technique can be used to measure the diffusion coefficient of oxygen molecules into these films quite accurately. At high PS content, diffusion of oxygen into composite film proceeded as a two-stage process, which can be explained with the existence of two different areas in the film. The results showed that diffusion of oxygen was reduced by increase in PS fraction. The low diffusion rate of oxygen in the composite is attributed to the formation of highly ordered almost void free PS phase in the composite film.

Our results were found consistent with the other studies reported in the literature for different composite systems. To our knowledge, no literature has reported the diffusion properties of PS/PNIPAM composites. In addition, this work has shown that fluorescence quenching technique provides a valuable method for investigating the oxygen diffusion into PS/PNIPAM composite films.

References

1. J. Jagur-Grodzinski: *Polym. Adv. Technol.*, 2006, **17**, 395.
2. J. K. Oh: *Can. J. Chem*, 2010, **88**, (3), 173.
3. J. Zhu: *Biomaterials*, 2010, **31**, (17), 4639.
4. B. V. Slaughter, S. S. Khurshid, O. Z. Fisher, A. Khademhosseini and N. A. Peppas: *Adv. Mater.*, 2009, **21**, (32-33), 3307.
5. D. Ratna and J. J. Karger-Kocsis: *Mater. Sci.*, 2008, **43**, 254.
6. F. Liu and M. W. Urban: *Prog. Polym. Sci.*, 2010, **35**, 3.
7. Z. M. O. Rzaev, S. Dincer and E. Piskin: *Prog. Polym. Sci.*, 2007, **32**, 534.
8. A. Sidorenko, T. Krupenkin, A. Taylor, P. Fratz and J. Aizenberg: *Science*, 2007, **315**, 487.
9. W. J. Zheng, N. An, J. H. Yang, J. Zhou and Y. M. Chen: *ACS Appl. Mater. Interfaces*, 2015, **28**, (7(3)), 1758.
10. Y. Y. Lui, Y. Yu, W. Tian, L. Sun and X. D. Fan: *Macromol. Biosci.*, 2009, **9**, (5), 525.
11. C. Yi and Z. Xu: *J. Appl. Polym. Sci.*, 2005, **96**, 824.
12. C. -L. Lin, W. -Y. Chiu and C. -F. Lee: *Polymer*, 2005, **46**, 10092.
13. B. V. Slaughter, S. S. Khurshid, O. Z. Fisher, A. Khademhosseini and N. A. Peppas: *Adv. Mater.*, 2009, **21**, (32–33), 3307.
14. C. R. Nuttelman, M. A. Rice, A. E. Rydholm, C. N. Salinas, D. N. Shah and K. S. Anseth: *Prog. Polym. Sci.*, 2008, **33**, (2), 167.
15. S. Varghese and J. H. Elisseeff: *Adv. Polym. Sci.*, 2006, **203**, 95.
16. R. M. Barrer: 'Diffusion in polymers', (eds. J. Crank and G. S. Park), 164–217; 1968, New York, Academic Press.
17. J. H. Koo: 'Polymer nanocomposites: processing, characterization, and applications'; 2006, New York, McGraw-Hill.
18. X. Lu, I. Manners and M. A. Winnik: *Macromolecules*, 2001, **34**, 1917.
19. R. K. Bharadwaj: *Macromolecules*, 2001, **34**, 9189.
20. J. P. Villaluenga, M. Khayet, M. A. Lopez-Manchado, J. L. Valentin, B. Seoane and J. I. Mengual: *Eur. Polym. J.*, 2007, **43**, (4), 1132.
21. W. Y. Wen: *Chem. Soc. Rev.*, 1993, **22**, 117.
22. M. E. Cox and B. Dunn: *J. Polym. Sci. Polym. Chem.*, 1986, **24**, 621.
23. M. E. Cox and B. Dunn: *J. Polym. Sci.*, 1986, **24**, 2395–2400.
24. J. R. MacCallum and A. L. Rudkin: *Eur. Polym. J.*, 1978, **14**, 655–656.
25. X. Lu, I. Manners and M. A. Winnik: 'Fluorescence spectroscopy; new trends in fluorescence spectroscopy', chap. 12, (eds. B. Valuer and J. C. Brochan), 229; 2001, New York, Springer-Verlag.
26. C. N. Jayarajah, A. Yekta, I. Manners and M. A. Winnik: *Macromolecules*, 2000, **33**, (15), 5693.
27. O. Pekcan and S. Ugur: *J. Coll. Interface Sci.*, 1999, **217**, 154–159.
28. O. Pekcan and S. Ugur: *Polymer*, 2000, **41**, 7531–7538.
29. S. Ugur, O. Yargi and O. Pekcan: *Appl. Clay Sci.*, 2009, **43**, 447.
30. O. Yargi, S. Ugur and O. Pekcan: *J. Fluoresc.*, 2013, **23**, 357.
31. S. Ugur, O. Yargi, A. Elaissari and O. Pekcan: *Macromol. Symp.*, 2009, **281**, 168.
32. O. Yargi, S. Ugur and O. Pekcan: *Polym. Eng. Sci.*, 2012, **52**, 172.
33. J. S. Liu, J. F. Feng and M. A. Winnik: *J. Chem. Phys.*, 1994, **101**, 9096.
34. F. Meunier and A. Elaissari: 'Poly(*N*-isopropylacrylamide)-based particles: preparation and colloidal characterization', in 'Surfactant science series' **115**, 117–144; 2003, New York, Marcel Dekker.
35. S. Ugur, O. Yargi and O. Pekcan: *Polym. Compos.*, 2008, **29**, 179.
36. O. Yargi, S. Ugur and O. Pekcan: *Polym. Adv. Technol.*, 2012, **23**, 776.
37. K. A. Kneas, J. N. Demas, B. Nguyen, A. Lockhart, W. Xu and B. A. DeGraff: *Anal. Chem.*, 2002, **74**, 1111.
38. A. Sorrentino, M. Tortora and V. Vittoria: *J. Polym. Sci. Polym. Phys.*, 2006, **44**, 265.
39. D. A. Pereira de Abreu, P. Paseiro Losada, I. Angulo and J. M. Cruz: *Eur. Polym. J.*, 2007, **43**, 2229.
40. T. C. Huang, C. F. Hsieh, T. C. Yeh, C. L. Lai, M. H. Tsai and J. M. Yeh: *J. Appl. Polym. Sci.*, 2011, **119**, 548.
41. M. E. Kose, R. J. Crutchley, M. C. DeRosa, N. Ananthakrishnan, J. R. Reynolds and K. S. Schanze: *Langmuir*, 2005, **21**, 8255.

Downloaded by [New York University] at 17:28 17 April 2016